communications chemistry

A Nature Portfolio journal

Article

https://doi.org/10.1038/s42004-025-01671-3

Gene conversion-associated successive engineering of modular polyketide synthases

Wenzheng Jin[1,2], Jiaming Tu[1,2], Bei Zhang[1,2], Xuri Wu[1,3] & Yijun Chen[1,2,3]

Modular polyketide synthases (PKSs) can produce various secondary metabolites in a collinearity fashion. Although rational engineering of modular PKS can ultimately create a diverse array of compounds, de novo generation of defined structures usually results in the loss or remarkable decline of productivity due primarily to the incompatibility of different elements. Here, we present a modular PKS engineering strategy driven by an evolutionary event of gene conversion to accomplish successive engineering of the modular PKS in cinnamomycin biosynthetic gene cluster (*cmm* BGC). By simulating the gene conversion process, *cmm* BGC is consecutively reprogrammed to generate a macrolide with predicted structural features. Moreover, the intra-module KS domain is demonstrated to associate with the proofreading of extender units. Collectively, the gene conversion-associated approach may shed a light on modular PKS engineering.

Polyketides are biosynthesized by polyketide synthases (PKSs) to possess remarkable structural diversities and valuable medicinal utilities[1]. Among different types of PKS, type I PKS functions in a modular fashion[2,3], in which the modules are linearly arranged to guide the unidirectional chain extension.

Since the early investigations on modular PKSs[4,5], the concept of "Lego-ization" in polyketide biosynthesis has continuously been evolved[6], allowing systematic reprogramming of PKSs to produce designed natural products with high stereo- and regio-specificity[7–9]. At the same time, various approaches, including site-directed mutagenesis, domain swapping and subunit insertions/deletions, have been implemented to the engineering of PKSs, aiming to side chain alteration or scaffold reconstruction. More recently, the strategies for PKS reprogramming have been moved forward from sequence-based design to structure-guided engineering[10,11]. However, the complex and dynamic conformations of PKSs[12–14], along with sophisticated interactions and functional interdependencies of different PKS domains[15,16], have posed considerable challenges for efficient engineering. Consequently, PKS assembly lines tend to become fragile following a single round of engineering, preventing successive reprogramming and applications[17].

The findings on the evolutionary events in modular PKSs[18], such as point mutation, gene duplication, gene loss, gene conversion, gene recombination, and horizontal gene transfer, have provided an opportunity for PKS engineering. In 2017, Abe lab proposed an evolutionary mechanism for structural diversification of polyketides by defining unique module organizations[19]. Keatinge-Clay lab demonstrated the improvement on success rate by using updated module boundaries for domain-fusion[20]. Based on the statistics of massive *trans*-AT PKS sequences, Piel lab applied the concept of evolutionary-guided engineering for *trans*-AT PKSs[21]. Collectively, the evolutionary information not only guides optimal recombination boundaries, but also facilitates the engineering efforts. For example, by simulating the evolutionary recombination of homologous modules, a ring-contracted mini-azalomycin was generated[22]. Regarding gene loss, the interconversions between polyene-pyrone structures, differing in the skeleton sizes, were accomplished[23,24]. Although engineering of PKS remains as a try-and-error, recent studies[25,26] mutually demonstrate that evolutionary events-guided engineering is broadly applicable, extending the scenarios beyond isolated and special cases.

Gene conversion is a prevalent evolutionary phenomenon observed in PKSs, whereby genetic material is exchanged between adjacent and homologous modules particularly between regions with high sequence similarity[27–29]. Thus, the event of gene conversion can alter specific regions for fine-tuning the chemical diversity of polyketides. This evolutionary event is widely distributed in *Streptomyces*, frequently occurring in KS and AT domains of modular PKS assembly lines according to nucleotide homolog and phylogenetic tree analyses[28–30]. Consequently, the gene conversion process is regarded as an important feature for the alteration of macrolide structure[28]. Meanwhile, the intra-module KS-AT didomain is found to often engage in gene conversion as a complete entity[25]. Nevertheless, although current knowledge on gene conversion is limited, emulating gene conversion events may offer a possibility of achieving successive PKS engineering.

[1]State Key Laboratory of Natural Medicines, China Pharmaceutical University, Nanjing, China. [2]Laboratory of Chemical Biology, College of Life Sciences and Technology, China Pharmaceutical University, Nanjing, China. [3]Department of Microbiology and Synthetic Biology, College of Life Sciences and Technology, China Pharmaceutical University, Nanjing, China. e-mail: yjchen@cpu.edu.cn

Previously, we unveiled an unusual type I/type III PKS hybrid *cmm* BGC and its products of cinnamomycin A-F (**1,1b, 1c** and **2–4**), a series of 14-membered macrolides with significant and selective anti-proliferative activity[31]. When we performed further analysis of *cmm* BGC, we found the presence of gene conversion with high homology or even identical DNA fragments in module 2, 6 and 7 (Fig. 1a, Supplementary Table 2). These regions are specifically located in malonyl-CoA-specific AT domains, spanning from C-terminus of KS domain to post-AT linker (Fig. 1b). The 100% nucleotide sequence identity of gene conversion region between modules 2 and 6 strongly supporting the connection of gene conversion with the biosynthesis of cinnamomycin skeleton. Therefore, previous successes in utilizing evolutionary approach for PKS engineering promoted us to test whether gene conversion process could be applied to empowering PKS engineering.

In this study, a homologous *mgm* BGC for possibly producing macrolides in *S. mangrovisoli*[32] was discovered by gene conversion-oriented genome mining. This homologous *mgm* BGC could be combined with *cmm* BGC to serve as a pair of templates for mimicking the process of gene conversion. By proposing an approach for emulating gene conversion process, successive engineering of the modular PKSs was accomplished in *cmm* BGC for de novo production of mangromycin-like compounds. Moreover, the intra-module KS domain was revealed to act as a proof-reading element for ensuring the fidelity of extender unit incorporation, expanding our knowledge on PKS synthetic logics.

Results

Discovery of a homologous *mgm* BGC by gene conversion-oriented genome mining

Bacterial natural products frequently exist as a large family of structural analogs, encoded by evolutionarily related homologous biosynthetic gene clusters. Similarly, the observation of gene conversion in *cmm* BGC could

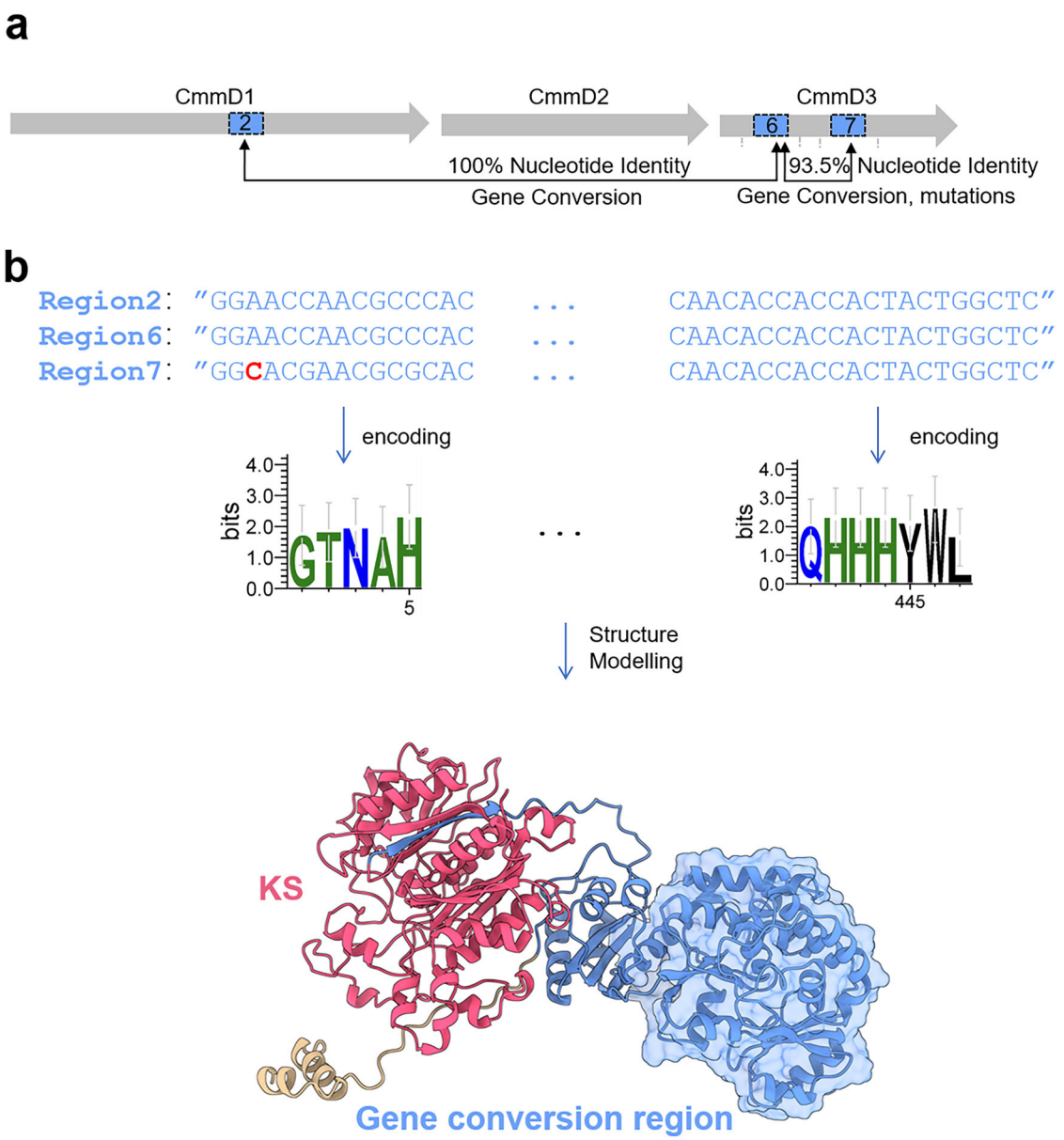

Fig. 1 | Identification of identical regions in *cmm* BGC and their structural features. a The locations of identical regions in *cmm* BGC. Rectangles colored in blue represent identical regions in CmmD1 and CmmD3. Numbers in rectangles are the abbreviation of module number; (**b**) The boundaries of gene conversion regions in module 2/6/7 and their encoding amino acid sequences are presented. Structural models of gene conversion regions in module 2/6/7 are created by AlphaFold 2.0. The regions colored in red represent the location neighboring KS domain; the portions colored in blue represent identical region; the part colored in brown represent post-AT region.

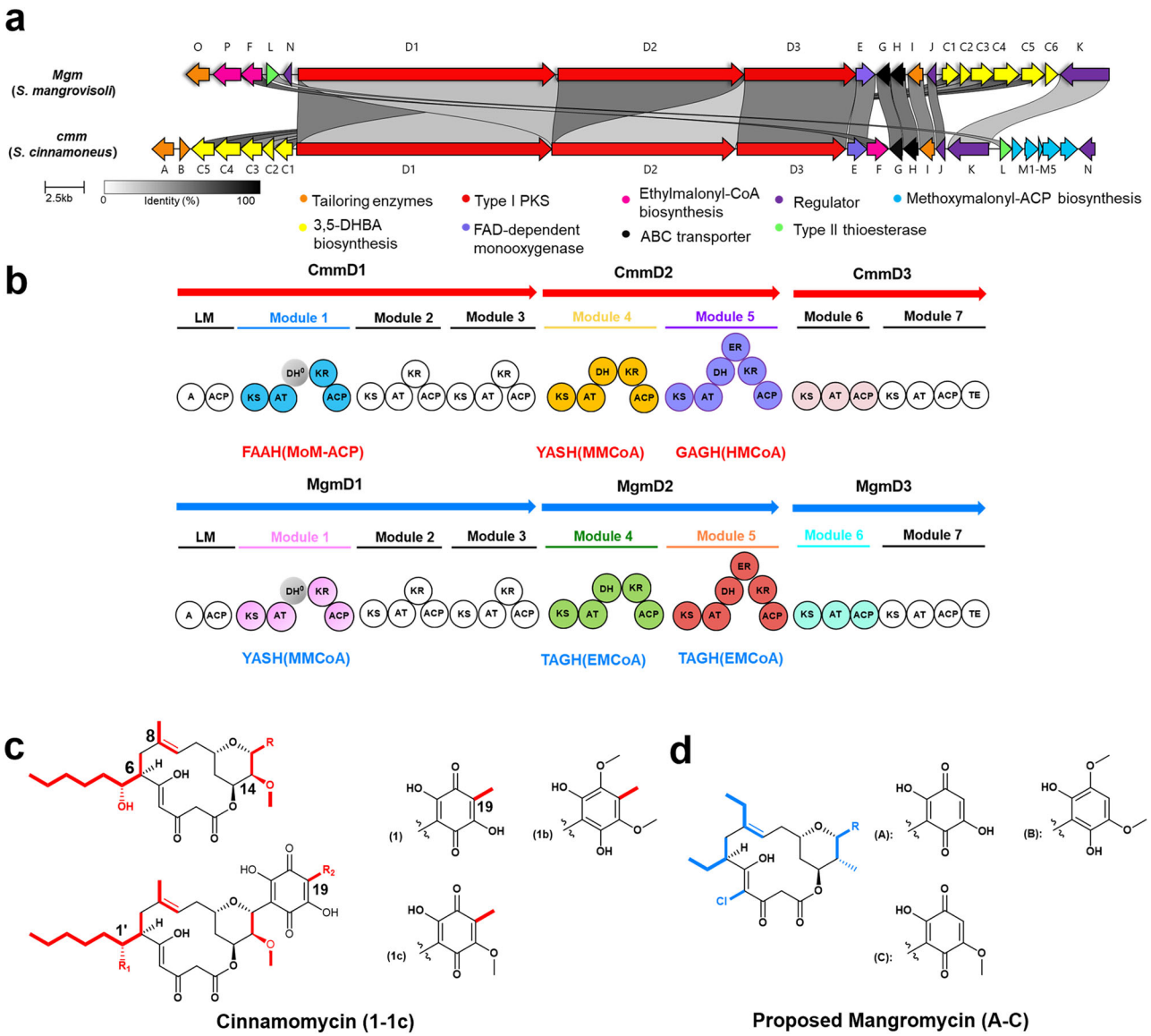

Fig. 2 | Comparisons of cinnamomycin and its BGC with *mgm* BGC and prediction of mangromycin structure. a Clinker analysis of *mgm* BGC and *cmm* BGC. Each ORF is labeled by a capital letter; (**b**) Domain organizations of *cmm* and *mgm* modular PKSs. Each circle represents a catalytic domain with its characteristic amino acid motif. The circles with the same color are originated from the same module. LM: 3,5-DHBA-specific loading module; DH^0: non-functional dehydratase domain. The signature motif "LAF" of CmmD1-DH^0 is present in MgmD1-DH^0 (Supplementary Fig. 4). Signature motifs for acyltransferase specificity with the corresponding extender unit are labeled under each module. OMM-ACP: methoxymalonyl-ACP; MMCoA: methylmalonyl-CoA; HMCoA: hexylmalonyl-CoA; EMCoA: ethylmalonyl-CoA. **c** Structures of cinnamomycins (**1, 1b, 1c**); (**d**) Proposed structures of mangromycin **A**-**C** based on the biosynthetic logic and bioinformatics analysis.

lead to the discovery of cinnamomycin-type compounds and their corresponding BGCs.

Since multiple ancestral cluster-specific fragments among homologous BGCs could be preserved by the process of gene conversion, these regions should be useful probes for genome mining. First, we used the gene conversion region in module2 of CmmD1 as the probe to mine BGC(s) with gene conversion characteristics in the NCBI genomic database. Unfortunately, the initial attempts did not yield any meaningful results, possibly due to a significant difference in sequence identity of AT domains caused by a large number of independent recombination events of AT domains in homologous BGCs. Since KS domains are usually accompanied with AT domains to possess gene conversion[26,28], this association encouraged us to use KS fragments in *cmm* BGC for a BLAST search. As a result, an uncharacterized homologous *mgm* BGC in *S. mangrovisoli* (GCF_000974985.2) was revealed (Supplementary Fig. 1). The products from this BGC were designated as mangromycins.

While *mgm* BGC shows significant similarity to *cmm* BGC (Fig. 2a, Supplementary Table 3 and Supplementary Figs. 2–5), notable differences do present, particularly the genes involved in the biosynthesis of extender units and tailoring steps (Fig. 2a). Specifically, a unique *mgmO* gene, encoding a phenol-type FAD-dependent halogenase[33], is located in the upstream of *mgm* BGC. After integration of *mgmO* gene in *cmm* BGC, chlorinated derivatives (**5–8**) were isolated and structurally elucidated. The structures of **5–8** revealed that the chlorination reaction took place at C4 position, whereas FAD-dependent halogenases typically undergo chlorination on the aromatic ring[33] (Additional descriptions are presented in the section of Materials and Methods, supplementary Figs. 6-10, and Supplementary Tables 3, 6–9). By contrast, the homologous genes of a P450

monooxygenase encoding *cmmA* and a methyltransferase encoding *cmmB* are not present in *mgm* BGC, suggesting distinct tailoring processes. Since the substrate specificity of AT domains determines the structural diversity of side chains, the differences of AT domains in the modules 1, 4, and 5 of *mgm* BGC were compared based on the signature motifs[2] (Supplementary Fig. 2). While MgmD1 is likely to incorporate methylmalonyl-CoA in module 1, MgmD2 might utilize ethylmalonyl-CoA in both modules 4 and 5, indicating acyl group variations between the skeletons of mangromycin and cinnamomycin (Fig. 2b). According to the biosynthetic logic and experimental evidence on the biosynthesis of cinnamomycin (Fig. 2c), we translated the genetic information of *mgm* BGC into possible structures of mangromycin **A**-**C** (Fig. 2d) along with a proposed biosynthetic pathway (Supplementary Fig. 11).

Thus, the high degree of similarity between *mgm* and *cmm* provided a platform for us to validate the PKS reprogramming approach. By emulating the process of gene conversion and employing a rational selection of the embedded elements and their boundaries, it might be possible to expand the application scope of PKS engineering.

Gene conversion-associated successive engineering to create mangromycin skeleton

Mangromycin and cinnamomycin exhibit slight variations in their side chains, which could be attributed to the occurrence of gene conversion processes within the AT regions. Therefore, we speculated that such structural transformations could be achieved through artificial mimicking of the process of gene conversion. To reprogram *cmm* BGC for producing predicted mangromycin, various extender units incorporated by modules 1, 4, and 5 in *cmm* BGC were individually altered for matching those in the corresponding regions of *mgm* BGC (Fig. 2b). To mimic the gene conversion process, we proposed following guidelines for AT engineering: (i) the DNA fragments spanning the regions from "GTNAH" to "HHYWL" in each module, highly homologous to the reported replacement boundaries for AT domain replacement[11,34], are designated as AT_c region to locate the boundaries. (ii) the prioritization of the catalytic elements should be from the same BGC; (iii) if the elements originated from other sources are selected to replace, high sequence homology to host BGCs should be a major consideration on the selection.

Following the guidelines (i) and (ii), we utilized the AT_c region from CmmD2-module 4, specific to methylmalonyl-CoA, to replace the corresponding region in CmmD1-module1, creating mutant S1 (Supplementary Table 4 and Supplementary Fig. 12), aiming to substitute the methoxy group by a methyl group at C14 (Fig. 3a).

In accordance with guideline iii), the MgmD2-AT_{5c} region showed higher homology to CmmD2-AT_{4c} than MgmD2-AT_{4c} region (55.28% vs. 50.55%). Thus, this region was chosen for the exchange with the corresponding region in module 4 of CmmD2 to generate mutant S2 (Supplementary Table 4 and Supplementary Fig. 13) or module 5 to produce mutant S3 (Supplementary Table 4 and Supplementary Fig. 14).

After the fermentation of mutant strains S1, S2, and S3, HPLC analyses (Fig. 3a) indicated the production of a series of peaks (**9–15a**) to display identical UV-Vis spectra to cinnamomycin **1** (Supplementary Fig. 15), along with the disappearance of cinnamomycin **1** and **2** in all mutants. Then, fermentation was scaled up for isolation and structural characterization. LC/MS and 1D and 2D NMR analyses (Supplementary Figs. 16–23 and Supplementary Tables 10–17) confirmed the structures of compounds **9–15a** (Fig. 3b). Compounds **9–12** from mutants S1 and S2 were in line with the alkyl group substitutions at C14 and C8 positions. Compared to **9** and **11**, compounds **10** and **12** lack a C1' hydroxyl group, due to lower catalytic activity of CmmA[31]. Notably, the yields of compounds **9–12** were not sacrificed, which was close to that of cinnamomycin **1** and **2** in wild-type strain (~50 mg/L).

Despite the utilization of Mgm-AT_5 region in both S2 and S3 strains, they surprisingly behaved significantly different (Fig. 3a). In S2 strain, Mgm-AT_5 region in module 4 resulted in ethyl substitution at C8 with high specificity. By contrast, S3 strain generated a group of structurally diverse cinnamomycin analogs **13a-15a**, varying in acyl groups at C6 position, whereas the desired product of **14a** was much less than expected. To enhance the biosynthesis of ethylmalonyl-CoA for improving the titer of **14a**, the genes of crotonyl-CoA carboxylase (CCR) and 3-hydroxybutyryl-CoA dehydrogenase (HCD) from *Streptomyces coelicolor* A3(2) (GCA_008931305.1), critical in the ethylmalonyl-CoA biosynthesis pathway[35], were inserted into pSET152, resulting in a construct of pSET152-CCR-HCD[36] (Supplementary Fig. 24). Subsequently, CCR and HCD was co-expressed in mutant S3, yielding S3-CCR-HCD mutant strain. Unexpectedly, although **14a** became the major product in the fermentation broth of S3-CCR-HCD strain (Fig. 3c), its titer remained comparable to that of S3 strain (~3 mg/L).

To further examine the feasibility for the creation of mangromycin skeleton under the direction of gene conversion, CmmD2-AT_4 in S1 strain was replaced by MgmD2-AT_5 to construct S4 strain (Supplementary Fig. 25). As expected, the S4 strain produced two compounds **16** and **17** at satisfactory titers (~15 mg/L). The structures of **16** and **17** were fully elucidated (Supplementary Figs. 26–27 and Supplementary Tables 18–19). Indeed, the substitutions at C8 and C14 took place to generate anticipated alkyl chains (Fig. 3d).

When CmmD2-AT_5 in S4 strain was substituted by MgmD2-AT_5, S5 strain was generated (Supplementary Fig. 25). However, different from S4 strain, HPLC-HRMS profiling of the fermentation broth of S5 strain showed six additional peaks (Fig. 3d). Following the scale-up fermentation of S5 strain and isolation, the structures of compounds **18b-c** and **19a-c** were characterized (Supplementary Figs. 28–29 and Supplementary Tables 20–24). Compounds **19a-c** contain a butyl chain attached at C6 position, whereas compounds **18b-c** feature desired ethyl substitution. Such a diversification of extender units in module 5 was similar to that in strain S3, indicating that AT domains are not the only elements for selective incorporation of extender units.

Identification of proofreading role of the intra-module KS domains for extender units

To increase the production of **18a-c**, we sought to elucidate the underlying mechanism that discriminates different acyl groups. Base on previous observation on the substrate specificity of AT domain in module 5, we speculated that the situation in S5 strain could be caused by unnatural domain-domain interactions from exogenous MgmD2-AT_5.

Theoretically, there could be three routes to decide extender unit specificity during chain extension (Fig. 4a–c). First, MgmD2-KS_5, as an intra-module KS, might function as a proof-reading element during the Claisen-condensation step[37]. Second, CmmD3-KS_6 might serve as a proofreader in the transfer of growing intermediates[38–40]. Third, the replacement of MgmD2-AT_5 might result in unnatural AT_5-ACP_5 interactions[41], affecting the fidelity of extender unit incorporation.

Next, to examine the actual route, we employed PKS domain counterparts from *mgm* BGC to replace internal elements for eliminating functional interferences from non-native domain-domain interactions. Additionally, through structural modeling by AlphaFold 2.0, the boundaries for the replacement of KS or ACP domains were precisely defined to ensure their compatibilities (Supplementary Figs. 30–32). Specifically, CmmD2-KS_5 was replace by its counterpart MgmD2-KS_5 from *mgm* BGC in S5 strain, resulting in S5-MgmKS_5 strain (Supplementary Figs. 33). Furthermore, S5-MgmKS_6 (Supplementary Fig. 34) and S5-MgmACP_5 (Supplementary Fig. 35) strains were similarly generated (Fig. 4d). After fermentation of these mutant strains, HPLC analyses revealed that S5-MgmKS_6 strain only produced trace amounts of **18a-c** and **19a-c** (Fig. 4), suggesting a low efficiency of the assembly line. On the other hand, S5-MgmACP_5 strain produced products equivalent to S5 strain with a similar ratio of **18a-c** and **19a-c**, implying that the interaction between non-cognate MgmD2-AT_5 and CmmD2-ACP_5 did not affect extender unit incorporation (Fig. 4d). Intriguingly, unlike the cases in S5-MgmKS_6 and S5-MgmACP_5, the production of desired macrolides **18a-c** was remarkably increased in the extracts of S5-MgmKS_5 strain, along with complete

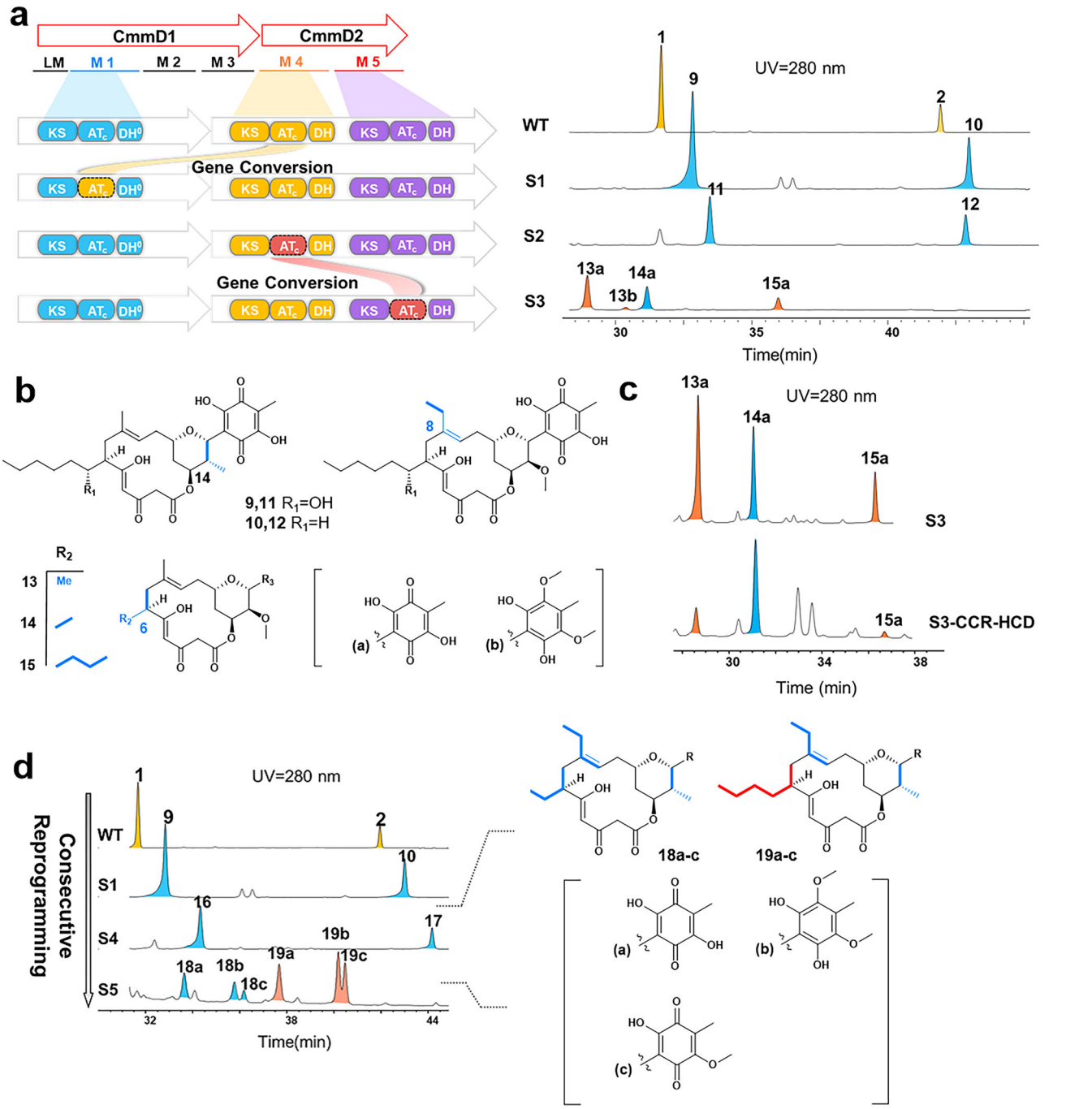

Fig. 3 | The generation of mangromycin scaffold by successive domain replacements. a Diagram for domain replacements in wild-type *S. cinnamoneus* (left) and HPLC analysis of different strains (right). Abbreviations represent different catalytic domains. AT$_c$ colored in yellow represent CmmD2-AT$_4$; AT$_c$ colored in red represent MgmD2-AT$_5$; (**b**) Structures of compounds **9–15a**; (**c**) HPLC analysis of strains of S3 and S3-CCR-HCD; **d** HPLC analysis of strains of S4 and S5 (left) and determined structures of the analogs (right).

abolishment of **19a-c** (Fig. 4d), implying the involvement of MgmKS$_5$ in the selection of extender units.

CmmD2-KS$_5$ and MgmD2-KS$_5$ shares 78.64% amino acid identity (Supplementary Fig. 36), but they possessed different specificity on extender units. This difference provided us an opportunity to identify the molecular basis in KS domains to determine the specificity. Multiple sequence alignments and structural modeling of these proteins indicated the presence of a specific region located near catalytically essential residues, which was previously named as "Active-Site Cap"[42,43] (Fig. 5). Based on the structure and location, we then speculated that the "Active-Site Cap" might be closely related to the specificity of KS domain towards extender unit. To test this hypothesis, a S5-ASC mutant strain was constructed (Supplementary Fig. 37), in which the "Active-Site Cap" of CmmD2-KS$_5$ was modified to match that of MgmD2-KS$_5$. Similar to the findings in S3-mgmKS$_5$ strain, the production of **19a-c** was completely abolished along with the accumulation of **18a-c** in S5-ASC strain (Fig. 5d), confirming that the specificity of KS domain on extender units is associated with the "Active Site Cap".

To pinpoint possible determinants for the specificity, amino acid residue 230 in KS domain, the position closest to catalytically essential residues within the "Active Site Cap", was identified to show difference between CmmD2-KS$_5$ and MgmD2-KS$_5$ (Fig. 5b). To demonstrate functional role of residue 230, site-directed mutagenesis was undertaken to

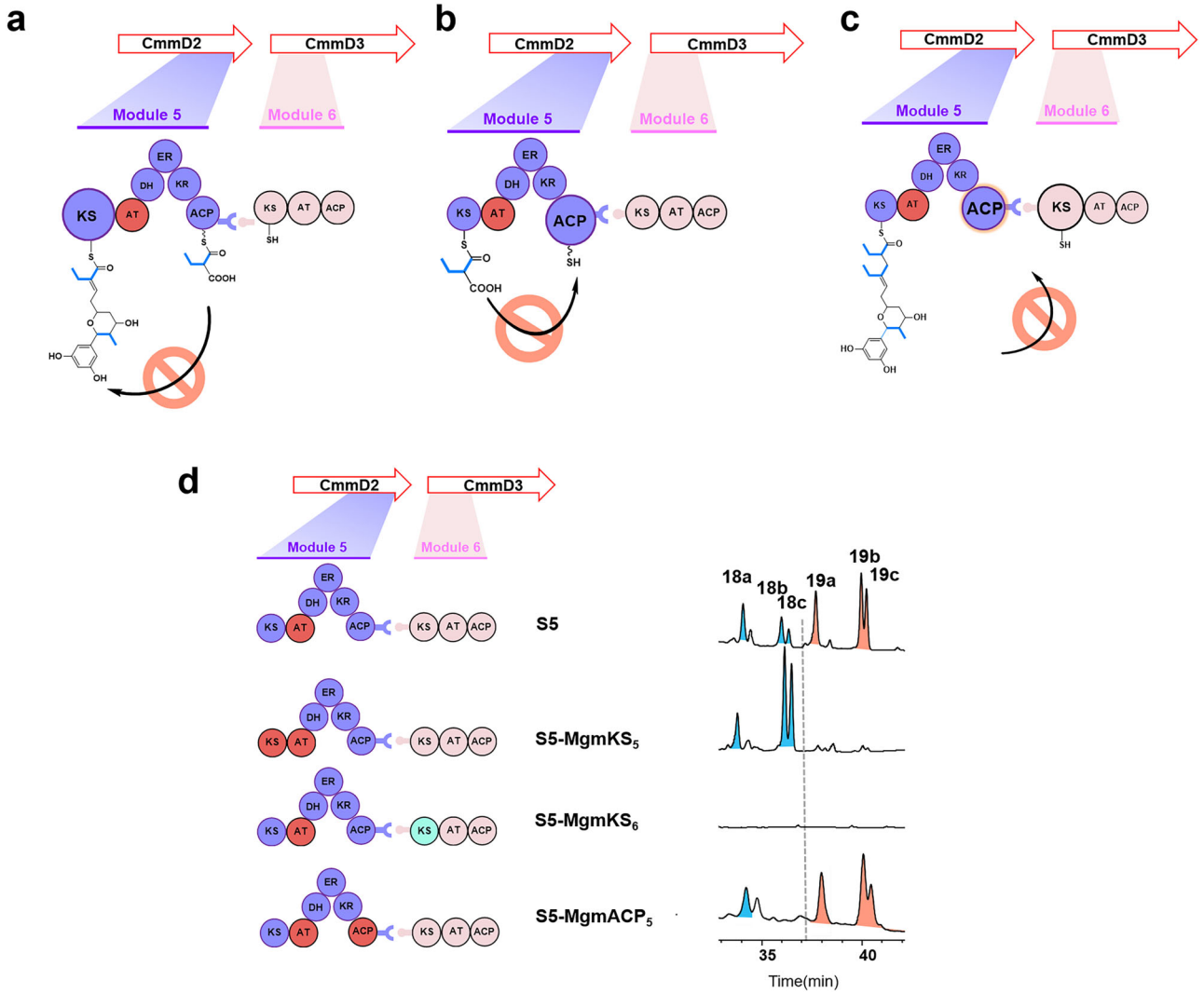

Fig. 4 | The creation of domain swap mutants for altering the specificity for extender units. a–c Potential routes and domain organizations for different extender units by domain swapping in S5 strain. Red circles represent exogenous MgmD2-$_{AT5}$, and purple and pink circles are natural domains in *cmm* BGC. ACP with red circle and KS with cyan circle indicate the counterpart domains from *mgm* BGC; (**d**) HPLC chromatograms of engineered strains at λ = 280 nm. The structures of **18a-c** and **19a-c** are shown in Fig. 3d along with their positions in HPLC analyses.

generate a mutant strain S3-A230T, where Ala was substituted by Thr in CmmD2-KS$_5$ domain (Supplementary Fig. 38). Consequently, a significant decrease of **19a-c** in the fermentation broth of S5-A230T strain (Fig. 5d) provided an evidence on the contribution of "Active Site Cap" of KS domain to the process of selecting a proper extender unit.

Biosynthesis of mangromycin C by systemic pathway reprogramming

With the establishment of macrolide skeleton (**18a-c**), complete biosynthesis of mangromycin required further engineering of tailoring steps. Since CmmA was unable to directly hydroxylate **18a-c**, the first step was to disrupt *cmmB* in S5-MgmKS$_5$ strain to yield S6 strain (Supplementary Fig. 39), thereby preventing the methylation at C19 (Fig. 6). Upon examining the fermentation broth of S6 strain, compound **20** was produced, but its yield was drastically decreased compared to **18a-c**. Consequently, sufficient amount of compound **20** was unable to obtain from 50 L fermentation, and its structure therefore was proposed by detailed HRMS/MS analysis (Supplementary Figs. 40 and 41).

According to the characteristics of flavin-dependent halogenase MgmO, C4-chlorination would be the final step to complete the biosynthesis of mangromycin. Given the extremely low abundance of compound **20** and chemical inversion upon the absence of methyl group, CCR-HCD dual gene fragments, was then inserted, under the control of independent *ermEp** promoter, into pSET152-mgmO plasmid to yield S7 strain (Supplementary Fig. 42). The fermentation of S7 strain led to the production of compound **21** (Supplementary Fig. 43). Following a 50 L fermentation, 1.5 mg of compound **21** was isolated for structural elucidation (Supplementary Table 25), confirming its structure as predicted mangromycin **C** (Fig. 2d and Fig. 6). Thus, through successive engineering efforts guided by the evolutionary event of gene conversion, a compound of mangromycin **C** was obtained by de novo construction of the biosynthetic pathway (Table 1).

In addition, a series of macrolides with diverse side chains were generated during the engineering processes (Table 1), which further exemplifies the functional compatibility and production efficiency in the present engineering.

Discussion

Polyketides biosynthesized by PKSs are a class important compounds with therapeutic values[44]. Currently, the emergence of drug-resistance and the growing demand for improved draggability have led to the need of structural diversity. The unique biosynthetic logics of modular PKSs provide an

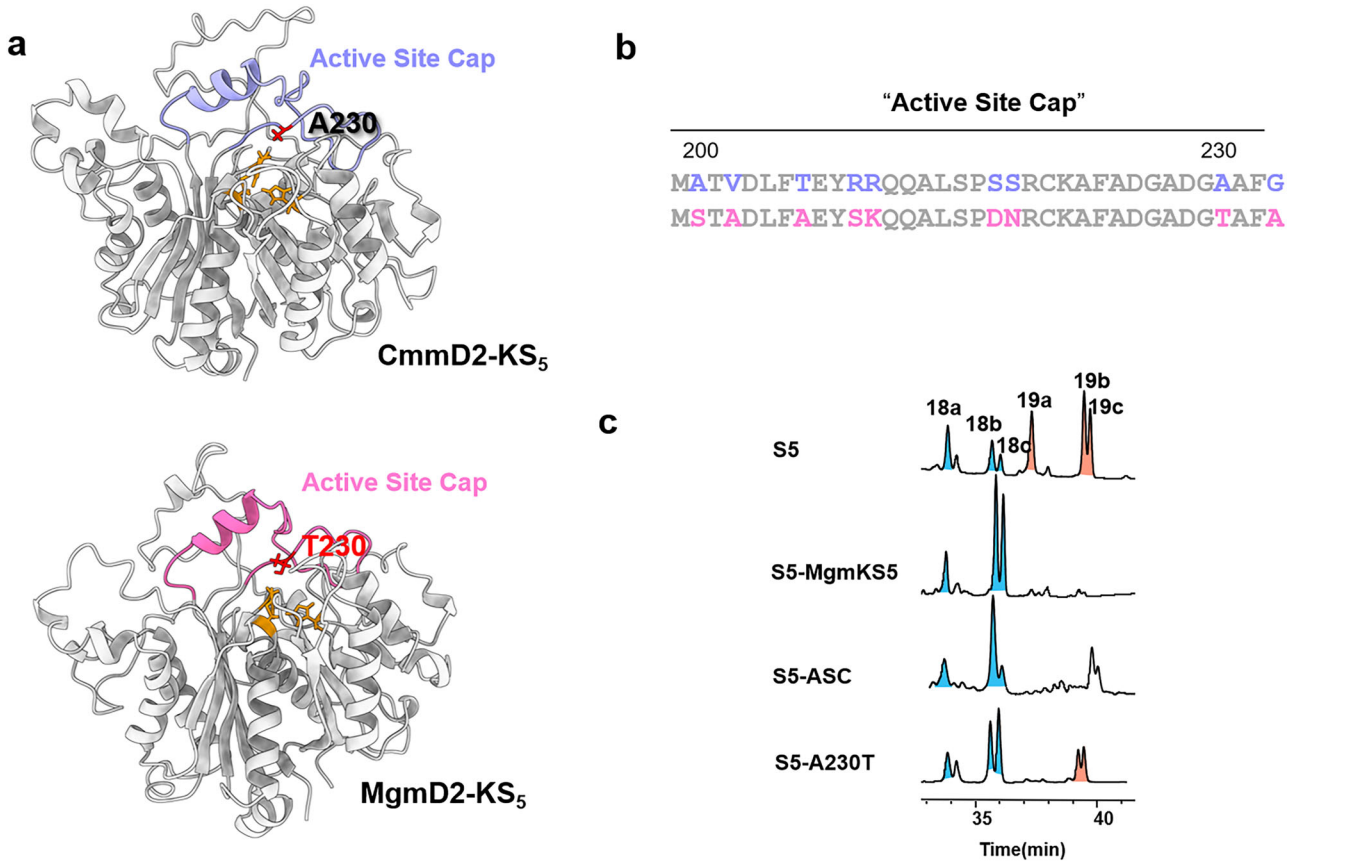

Fig. 5 | "Active Site Cap" region of KS domain contributed to the extender unit specificity. a Structural models of CmmD2-KS_5 and MgmD2-KS_5 created by using AlphaFold 2.0. The catalytic essential residues are colored in yellow with the indication of residues 230; (**b**) Sequence comparison of "Active Site Cap" region of CmmD2-KS_5 and MgmD2-KS_5; (**c**) HPLC chromatograms of engineered strains with the same treatments and amounts of fermentation broth at λ = 280 nm with three independent repeats.

opportunity to utilize synthetic biology approach to reprogram PKSs. However, the production of structural analogs by conventional PKS reprogramming is still in the stage of trial-and-correct, due primarily to insufficient knowledge on dynamic conformations of different modules, domain-domain interactions, and speed-limiting bottlenecks in the complex biosynthetic processes.

Inspired by nature's creation of diverse PKSs and their biosynthetic pathways, evolution-oriented strategies have shown the usefulness and promise in PKS engineering. For instance, mimicking and accelerating natural evolution in laboratory settings for modular PKSs have been practiced to yield various families of polyketides with high yields, such as ring-contracted or ring-expanded rapamycins[27]. Meanwhile, evolution-related PKS engineering approaches possess the capability of refining the assembly lines in well-organized and coordinated modular PKSs. Additionally, natural evolution contributes to the guidance of optimal selection of splice points during the designs for PKS engineering. Recent reports have extensively demonstrated that the modular unit for insertion or deletion can adhere to a "redefined module"[19,20], spanning from upstream AT to downstream KS, rather than following canonical order from KS to ACP.

With the development of combinational biosynthesis, successive PKS engineering has emerged as a frontier to achieve double or even triple substitutions to produce "unnatural" natural products[45]. However, unpredictable functionality of chimeric assembly line and historically low yield by domain swapping have continuously hindered efficient PKS engineering because of the compatibility issues associated with sequence, structure and function. Similar to the other evolutionary process observed in PKSs, gene conversion has been observed and proposed to occur at a high frequency in regions containing AT domains or KS domains, and the gene conversion process is thought to enable structure diverse in polyketide skeletons. Despite the success on successive engineering in this study, the replacements of different regions of AT domains still exhibited noticeable differences, which reflects the complexity of PKS assembly lines influenced by various factors. Thus, further investigation on the rationale on compatibility and selection criteria will be required.

In this study, we confirmed a piece of evidence for gene conversion occurred in the AT domain of the cmm BGC, which may reflect how nature creates the diversity of acyl groups through certain evolutionary events like gene conversion. Subsequent genome mining resulted in the identification of a homologous *mgm* BGC containing gene conversion, which enabled us to test the usefulness of gene conversion-associated approach for PKS engineering. Specifically, our approach focused on selecting highly compatible fragments and the boundaries of AT and KS domains by imitating the process of gene conversion. After validating the approach, we performed a series of gene conversion-associated engineering to create a line of chimeric assemblies with four-fold substitution for the generation of a series of cinnamomycin derivatives.

Commonly, the quality control system of modular PKSs consists of a series of coordinated events to ensure irreversible assembly of substrate and the rate of product output. This system includes the dictation of the flow of inter-modular substrate transfer by docking domain pairing[46], the gatekeeping roles of downstream KS domains and the hydrolysis of inaccurate intermediates by type II thioesterases[47]. On the other hand, it is also observed that some PKSs, such as the ones producing antimycin or epothilone, display a tolerance to incorporate different extender units, often attributing to substrate promiscuity of AT domain. Regardless of various outcomes, the precise mechanism on ensuring the fidelity of extender units during

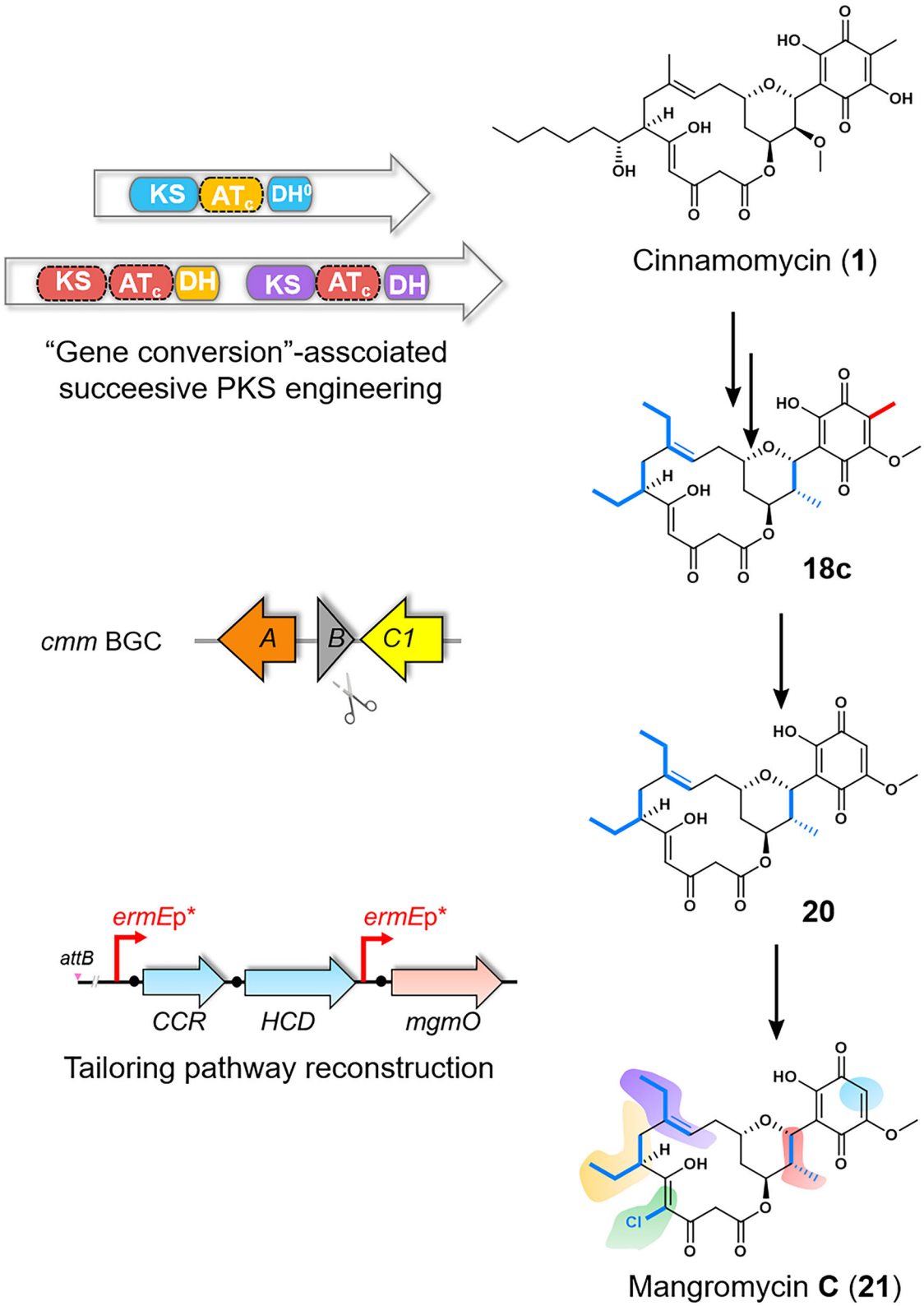

Fig. 6 | Establishing the biosynthetic route of mangromycin C (21) by de novo engineering in *Streptomyces cinnamoneus*. Proposed biosynthetic route of mangromycin **C** generated using *S. cinnamoneus* as a template. The gray triangle labeled **B** represents the in-frame deletion of *cmmB* gene in S5-mgmKS$_5$ strain. The arrows labeled in **A** and **C1** represent the open reading frames of *cmmA* and *cmmC1*.

Claisen-condensation step is not fully elucidated. In this study, we identified the proofreading role of intra-module KS domains to control the fidelity of extender units, providing a possibility for the governance of polyketide synthase assembly line and the involvement of KS-AT didomain. Recently, the condensation domain in NRPS biosynthesis was also revealed to be proofreading for the control of substrate- and stereo-specificity[48], suggesting a notable fashion of proofreading for well-coordinated stepwise biosynthesis of natural products. Therefore, because of the pivotal roles in determining substrate specificity and stereochemistry, organizational and functional characteristics of intra-module KS domains may largely decide the outcomes of PKS reprogramming.

In the past decades, the discovery of clinically useful molecules has been one of the major tasks in the field of natural product research[49]. However, some BGCs for producing natural products are virtually inaccessible regardless of the advancement of various tools for activating cryptic BGCs, thus limiting the access to the vast chemical space. Recent combination of genome mining with chemical synthesis resulted in a NRPS-like molecule, leading to the identification of an antibiotic capable of bypassing drug resistance[50]. The present work also showed that, the precise reprogramming of known biosynthetic pathways could be a feasible approach to obtain targeted molecules, which might be a valuable addition to the discovery of bioactive natural products.

Conclusions

In the present study, we have accomplished successive engineering of PKSs for targeted generation of polyketides based on the evolutionary event of gene conversion typically occurred in KS and AT domains. This approach has led to the creation of an artificial PKS gene cluster to produce a new-to-nature compound of mangromycin C. Moreover, we have demonstrated that the selectivity of extender units within the module is governed by intra-module KS domain, rather than previously proposed by AT domain alone. The present PKS engineering associated with gene conversion may facilitate the discovery of bacterial natural products and provide insights into the correlation between PKS biosynthetic rationale and evolutionary feature.

Materials and methods

Culture conditions and media

Streptomyces cinnamoneus ATCC 21532 and its mutant were cultured on solid ISP2 medium (4 g/L yeast extract, 4 g/L glucose, 10 g/L malt extract, 20 g/L agar) at 30 °C for 4 days for sporulation. Fresh spores of *S. cinnamoneus* were inoculated into 50 mL seed medium (15 g/L glucose, 2 g/L casamino acid, 1 g/L yeast extract, 1 g/L beef extract). After 3-day growth, SPC medium (40 g/L soybean meal, 30 g/L potato starch, 4 g/L $CaCO_3$) was used for the fermentation of S. cinnamoneus at 30 °C, 220 rpm for 7 days.

Characterization of FAD-dependent halogenase mgmO to catalyze an unexpected olefin chlorination

To characterize the flavin-dependent halogenases (FDHs) are recognized for their capability to incorporate halogens into natural products, which are further categorized into subclasses based on their substrate-specificity and sequence homology. A phylogenetic comparison of MgmO in *mgm* BGC with known FDHs indicated that MgmO falls in the phenolic-type FDHs, known to chlorinate phenolic moieties (Supplementary Fig. 6). Accordingly, it was reasonable to speculate that MgmO catalyzes the chlorination at C19 position of 2,5-dihydroxy-*p*-benzoquinone moiety in cinnamomycins (Supplementary Fig. 8a), the site also to be methylated by CmmB. To examine the function of MgmO, the gene of *mgmO* was synthesized (Supplementary Table 2) and incorporated into pSET152 under the control of constitutive *ermE**p promoter (Supplementary Table 4 and Supplementary Fig. 7). To eliminate potential interference from CmmB, pSET152-mgmO construct was introduced into wild-type *S. cinnamoneus* and*ΔcmmB* mutant, resulting in the strains of WT-mgmO and ΔcmmB-mgmO for heterologous expression of *mgmO*. After fermentation of these strains, HPLC analyses showed the appearance of four peaks (Supplementary Fig. 8b), which were confirmed as chlorinated derivatives of cinnamomycin **1**–**4** based on their MS fragmentations (Supplementary Figs. 9 and 10). Surprisingly, the chlorination occurred at C4 position of the double bond in cinnamomycins after structural elucidation of compounds **5**–**8** from large-scale fermentation, purification and NMR spectroscopy (Supplementary Tables 6–9). The chlorination at the same position by the strains of WT-mgmO and ΔcmmB-mgmO further ruled out the possibility of competing for C19 position. Thus, the function of MgmO was characterized as a FAD-dependent halogenase to chlorinate the olefin group of cinnamomycin-type macrolides (Supplementary Fig. 8a).

Table 1 | Structural analogs generated during the successive engineering

Strain	Compound	Production Yield[a]	Construction method
Wild-type (*S.cinnamoneus*)	**1**[b]	~50 mg/L	N/A[c]
	1b	~2 mg/L	
	1c	~1 mg/L	
	2	~10 mg/L	
ΔcmmB	**3**	~50 mg/L	*cmmB* in-frame deletion mutant[2]
	4	~10 mg/L	
WT+mgmO	**5**	~10 mg/L	*mgmO* gene integrated strain of WT
	6	~2 mg/L	
ΔcmmB+mgmO	**7**	~10 mg/L	*mgmO* gene integrated strain of ΔcmmB mutant
	8	~2 mg/L	
S1	**9**	~50 mg/L	Cmm-AT_1 replacement mutant with Cmm-AT_4 in WT
	10	~15 mg/L	
S2	**11**	~30 mg/L	Cmm-AT_4 replacement mutant with Mgm-AT_5 in WT
	12	~7 mg/L	
S3	**13a**	~5 mg/L	Cmm-AT5 replacement mutant with Mgm-AT_5 in WT
	13b	~0.5 mg/L	
	14a	~3 mg/L	
	15a	~2 mg/L	
S4	**16**	~15 mg/L	Cmm-AT_4 replacement mutant with Mgm-AT_5 in S3
	17	~3 mg/L	
S5	**18a**	~2 mg/L	Cmm-AT5 replacement mutant with Mgm-AT_5 in S4
	18b	~1.5 mg/L	
	18c	~0.5 mg/L	
	19a	~4 mg/L	
	19b	~5 mg/L	
	19c	~5 mg/L	
S5-mgmKS_5	**18a**	~1.5 mg/L	Cmm-KS_5 replacement mutant with Mgm-KS_5 in S5
	18b	~4 mg/L	
	18c	~4 mg/L	
S6	**20**	Trace	*cmmB* in-frame deletion mutant in S5-mgmKS_5
S7	**21**	~0.5 mg/L	CCR-HCD- mgmO co-overexpression in mutant S6

a: The production yield was estimated by integrating the peak area under UV 280 nm compared to compound **1** or isolated amount;
[b]Bold style represents compound name in number;
[c]not applicable.

Genetic manipulations

The plasmid pSET152-mgmO was used to construct the integrated mutant WT-mgmO and ΔcmmB-mgmO in vivo. Firstly, fragment of *ermE**p-*mgmO* were synthesized by GenScript Biotechnology Co., Ltd (Nanjing, China). Then, the fragment was inserted into the *Eco*RI and *Eco*RV sites of *Streptomyces-E. coli* shuttle vector pSET152 to generate the plasmid pSET152-mgmO using T4 DNA ligase. Similar procedures are performed to obtain other plasmids pSET152-CCR-HCD and pSET152-CCR-HCD-mgmO, summarized in Supplementary Fig. 7 and Supplementary Table 4. All plasmids were sequenced and verified.

The plasmid pKC1139-S1 was used to construct the domain replacement mutant S1 in vivo. Firstly, two homologous fragments flanking gene conversion region in CmmD1-module 1 were amplified from *S. cinnamoneus* genome DNA by two pairs of primers S1-P1 and S1-P2, S1-P5 and S1-P6. Then, gene conversion region in CmmD2-module 4 were amplified from *S. cinnamoneus* genome DNA by primers S1-P3 and S1-P4. Then, these three fragments were inserted into the *Eco*RI and HindIII sites of *Streptomyces-E. coli* shuttle vector pKC1139 to generate the plasmid pKC1139-S1 using In-fusion cloning kit. Similar procedures are performed to obtain other plasmids for domain replacement mutants or in-frame deletion mutant, summarized in Supplementary Table 5. All plasmids were sequenced and verified.

Using mutant strain S1 as an example, the constructed plasmid pKC1139-S1 was transformed into the donor strain *E. coli* ET12567/pUZ8002. After *E. coli-Streptomyces* conjugation, and then apramycin-resistant ex-conjugants were incubated in ISP2 medium at 30 °C to generate double-crossover mutant. A pair of primers S1-C1 and S1-C2 was used to obtain the gene fragments, and PCR products were sequentially digested by *Not*I restriction enzyme and sequenced. Similar procedures were performed to obtain other mutant strains (Supplementary Figs. 12–14, 25, 33–35 and 37–39).

Isolation and purification of cinnamomycin analogues 5-21

For isolation of compounds **5** and **6** from strain WT+mgmO (Supplementary Table 4), a total of 5 L of fermentation media were extracted with an equal volume of ethyl acetate. The extracts were evaporated and dissolved in ethyl acetate. Then, the crude extracts were subjected to C18 silica gel column chromatography, and eluted stepwise using an acetonitrile/water gradient from 10% acetonitrile to 100% acetonitrile. The fractions containing the target compounds were confirmed by HPLC analyses, and the same fractions were combined. Finally, 80 mg of **5** and 60 mg of **6** was obtained.

Compound **5**: yellow powder. NMR data, see Supplementary Table 6.

Compound **6**: yellow powder. NMR data, see Supplementary Table 7.

For isolation of compounds **7** and **8** from strain ΔcmmB+mgmO (Supplementary Table 4), a total of 5 L of fermentation media were extracted with an equal volume of ethyl acetate. The extracts were evaporated and dissolved in ethyl acetate. Then, the crude extracts were subjected to C18 silica gel column chromatography, and eluted stepwise using an acetonitrile/water gradient from 10% acetonitrile to 100% acetonitrile. The fractions containing the target compounds were confirmed by HPLC analyses, and the same fractions were combined. Finally, 70 mg of **7** and 50 mg of **8** was obtained.

Compound **7**: yellow powder. NMR data, see Supplementary Table 8.

Compound **8**: yellow powder. NMR data, see Supplementary Table 9.

For isolation of compounds **9** and **10** from strain S1 (Supplementary Table 5), a total of 3 L of fermentation media were extracted with an equal volume of ethyl acetate. The extracts were evaporated and dissolved in ethyl acetate. Then, the crude extracts were subjected to C18 silica gel column chromatography, and eluted stepwise using an acetonitrile/water gradient from 10% acetonitrile to 100% acetonitrile. The fractions containing the target compounds were confirmed by HPLC analyses, and the same fractions were combined. Finally, 180 mg of **9** and 60 mg of **10** was obtained.

Compound **9**: yellow powder. NMR data, see Supplementary Table 10.

Compound **10**: yellow powder. NMR data, see Supplementary Table 11.

For isolation of compounds **11** and **12** from strain S2 (Supplementary Table 5), a total of 3 L of fermentation media were extracted with an equal volume of ethyl acetate. The extracts were evaporated and dissolved in ethyl acetate. Then, the crude extracts were subjected to C18 silica gel column chromatography, and eluted stepwise using an acetonitrile/water gradient from 10% acetonitrile to 100% acetonitrile. The fractions containing the target compounds were confirmed by HPLC analyses, and the same fractions were combined. Finally, 75 mg of **11** and 35 mg of **12** was obtained.

Compound **11**: yellow powder. NMR data, see Supplementary Table 12.

Compound **12**: yellow powder. NMR data, see Supplementary Table 13.

For isolation of compounds **13a, 13b, 14a** and **15a** from strain S3 (Supplementary Table 5), a total of 15 L of fermentation media were extracted with an equal volume of ethyl acetate. The extracts were evaporated and dissolved in ethyl acetate. Then, the crude extracts were subjected to C18 silica gel column chromatography, and eluted stepwise using an acetonitrile/water gradient from 10% acetonitrile to 100% acetonitrile. The fractions containing the target compounds were confirmed by HPLC analyses, and the same fractions were combined. Fractions containing the desired compounds were further purified using semi-preparative HPLC on a YMC-Pack ODS-A column with a water/acetonitrile gradient (35:65) over 25 min at a flow rate of 1.0 mL/min monitored at 280 nm. Finally, 75 mg of **13a**, 7.5 mg of **13b**, 30 mg of **14a** and 20 mg of **15a** was obtained.

Compound **13a**: yellow powder. NMR data, see Supplementary Table 14.

Compound **13b**: white powder. NMR data, see Supplementary Table 15.

Compound **14a**: yellow powder. NMR data, see Supplementary Table 16.

Compound **15a**: yellow powder. NMR data, see Supplementary Table 17.

For isolation of compounds **16** and **17** from strain S4 (Supplementary Table 5), a total of 3 L of fermentation media were extracted with an equal volume of ethyl acetate. The extracts were evaporated and dissolved in ethyl acetate. Then, the crude extracts were subjected to C18 silica gel column chromatography, and eluted stepwise using an acetonitrile/water gradient from 10% acetonitrile to 100% acetonitrile. The fractions containing the target compounds were confirmed by HPLC analyses, and the same fractions were combined. Finally, 75 mg of **16** and 30 mg of **17** was obtained.

Compound **16**: yellow powder. NMR data, see Supplementary Table 18.

Compound **17**: yellow powder. NMR data, see Supplementary Table 19.

For isolation of compounds **18b and 18c** from strain S5-mgmKS_5 (Supplementary Table 5), a total of 10 L of fermentation media were extracted with an equal volume of ethyl acetate. The extracts were evaporated and dissolved in ethyl acetate. Then, the crude extracts were subjected to C18 silica gel column chromatography, and eluted stepwise using an acetonitrile/water gradient from 10% acetonitrile to 100% acetonitrile. The fractions containing the target compounds were confirmed by HPLC analyses, and the same fractions were combined. Fractions containing the desired compounds were further purified using semi-preparative HPLC on a YMC-Pack ODS-A column with a water/acetonitrile gradient (35:65) over 25 min at a flow rate of 1.0 mL/min monitored at 280 nm. Compound **18a** degrades during purification process. Finally, 35 mg of **18b** and 30 mg of **15a** was obtained.

Compound **18b**: white powder. NMR data, see Supplementary Table 20.

Compound **18c**: yellow powder. NMR data, see Supplementary Table 21.

For isolation of compounds **19a, 19b** and **19c** from strain S5 (Supplementary Table 5), a total of 10 L of fermentation media were extracted

with an equal volume of ethyl acetate. The extracts were evaporated and dissolved in ethyl acetate. Then, the crude extracts were subjected to C18 silica gel column chromatography, and eluted stepwise using an acetonitrile/water gradient from 10% acetonitrile to 100% acetonitrile. The fractions containing the target compounds were confirmed by HPLC analyses, and the same fractions were combined. Fractions containing the desired compounds were further purified using semi-preparative HPLC on a YMC-Pack ODS-A column with a water/acetonitrile gradient (15:85) over 25 min at a flow rate of 1.0 mL/min monitored at 280 nm. Finally, 25 mg of **19a**, 20 mg of **19b** and 25 mg of **19c** was obtained.

Compound **19a**: yellow powder. NMR data, see Supplementary Table 22.

Compound **19b**: white powder. NMR data, see Supplementary Table 23.

Compound **19c**: yellow powder. NMR data, see Supplementary Table 24.

For isolation of compound **21** from strain S7 (Supplementary Table 5), a total of 20 L of fermentation media were extracted with an equal volume of ethyl acetate. The extracts were evaporated and dissolved in ethyl acetate. Then, the crude extracts were subjected to C18 silica gel column chromatography, and eluted stepwise using an acetonitrile/water gradient from 10% acetonitrile to 100% acetonitrile. Compound **21** easily dispersed on the column, so that we increased the column pressure during the purification process. The fractions containing the **21** were confirmed by HPLC analyses, and the same fractions were combined. Fractions containing the desired compounds were further purified using semi-preparative HPLC on a YMC-Pack ODS-A column with a water/acetonitrile gradient (35:65) over 25 min at a flow rate of 1.0 mL/min monitored at 280 nm. Finally, 3.5 mg of **21** was obtained.

Compound **21**: yellow powder. NMR data, see Supplementary Table 25.

Reporting summary

Further information on research design is available in the Nature Portfolio Reporting Summary linked to this article.

Data availability

Data supporting the findings of this work are available within the paper and Supplementary Information files. Experimental information, supporting tables and figures are available in Supplementary Information (PDF). Supplementary Data (NMR spectra) can be found in the separate file (PDF). Further information on research design is available in the Nature Research Reporting Summary linked to this article.

Received: 25 June 2025; Accepted: 20 August 2025;
Published online: 27 August 2025

References

1. Hertweck, C. The biosynthetic logic of polyketide diversity. *Angew. Chem. Int. Ed.* **48**, 4688–4716 (2009).
2. Keatinge-Clay, A. T. The structures of type I polyketide synthases. *Nat. Prod. Rep.* **29**, 1050–1073 (2012).
3. Smith, S. & Tsai, S. C. The type I fatty acid and polyketide synthases: a tale of two megasynthases. *Nat. Prod. Rep.* **24**, 1041–1072 (2007).
4. Cortes, J., Haydock, S. F., Roberts, G. A., Bevitt, D. J. & Leadlay, P. F. An unusually large multifunctional polypeptide in the erythromycin-producing polyketide synthase of *Saccharopolyspora erythraea*. *Nature* **348**, 176–178 (1990).
5. Donadio, S. et al. Modular organization of genes required for complex polyketide biosynthesis. *Science* **252**, 675–679 (1991).
6. Sherman, D. H. The Lego-ization of polyketide biosynthesis. *Nat. Biotechnol.* **23**, 1083–1084 (2005).
7. Keatinge-Clay, A. T. Stereocontrol within polyketide assembly lines. *Nat. Prod. Rep.* **33**, 141–149 (2016).
8. Weissman, K. J. & Leadlay, P. F. Combinatorial biosynthesis of reduced polyketides. *Nat. Rev. Microbiol.* **3**, 925–936 (2005).
9. Weissman, K. J. Genetic engineering of modular PKSs: from combinatorial biosynthesis to synthetic biology. *Nat. Prod. Rep.* **33**, 203–230 (2016).
10. Su, L. et al. Engineering the stambomycin modular polyketide synthase yields 37-membered mini-stambomycins. *Nat. Commun.* **13**, 515 (2022).
11. Nava, A. A., Roberts, J., Haushalter, R. W., Wang, Z. & Keasling, J. D. Module-based polyketide synthase engineering for de novo polyketide biosynthesis. *ACS Synth. Biol.* **12**, 3148–3155 (2023).
12. Whicher, J. R. et al. Structural rearrangements of a polyketide synthase module during its catalytic cycle. *Nature* **510**, 560–564 (2014).
13. Dutta, S. et al. Structure of a modular polyketide synthase. *Nature* **510**, 512–517 (2014).
14. Cogan, D. P. et al. Mapping the catalytic conformations of an assembly-line polyketide synthase module. *Science* **374**, 729–734 (2021).
15. Xu, W., Qiao, K. & Tang, Y. Structural analysis of protein-protein interactions in type I polyketide synthases. *Crit. Rev. Biochem. Mol. Biol.* **48**, 98–122 (2013).
16. Dodge, G. J., Maloney, F. P. & Smith, J. L. Protein-protein interactions in "*cis*-AT" polyketide synthases. *Nat. Prod. Rep.* **35**, 1082–1096 (2018).
17. Klaus, M. & Grininger, M. Engineering strategies for rational polyketide synthase design. *Nat. Prod. Rep.* **35**, 1070–1081 (2018).
18. Nivina, A., Yuet, K. P., Hsu, J. & Khosla, C. Evolution and diversity of assembly-line polyketide synthases. *Chem. Rev.* **119**, 12524–12547 (2019).
19. Zhang, L. et al. Characterization of giant modular PKSs provides insight into genetic mechanism for structural diversification of aminopolyol polyketides. *Angew. Chem. Int. Ed.* **56**, 1740–1745 (2017).
20. Miyazawa, T., Hirsch, M., Zhang, Z. & Keatinge-Clay, A. T. An in vitro platform for engineering and harnessing modular polyketide synthases. *Nat. Commun.* **11**, 80 (2020).
21. Mabesoone, J. et al. Evolution-guided engineering of trans-acyltransferase polyketide synthases. *Science* **383**, 1312–1317 (2024).
22. Zhai, G. et al. Insights into azalomycin F assembly-line contribute to evolution-guided polyketide synthase engineering and identification of intermodular recognition. *Nat. Commun.* **14**, 612 (2023).
23. Sugimoto, Y., Ding, L., Ishida, K. & Hertweck, C. Rational design of modular polyketide synthases: morphing the aureothin pathway into a luteoreticulin assembly line. *Angew. Chem. Int. Ed.* **53**, 1560–1564 (2014).
24. Peng, H., Ishida, K., Sugimoto, Y., Jenke-Kodama, H. & Hertweck, C. Emulating evolutionary processes to morph aureothin-type modular polyketide synthases and associated oxygenases. *Nat. Commun.* **10**, 3918 (2019).
25. Ray, K. A. et al. Assessing and harnessing updated polyketide synthase modules through combinatorial engineering. *Nat. Commun.* **15**, 6485 (2024).
26. Huang, Z. et al. Plug-and-play engineering of modular polyketide synthases. *Nat. Chem. Bio.* https://doi.org/10.1038/s41589-025-01878-4 (2025).
27. Wlodek, A. et al. Diversity oriented biosynthesis via accelerated evolution of modular gene clusters. *Nat. Commun.* **8**, 1206 (2017). **2017**.
28. Zucko, J., Long, P. F., Hranueli, D. & Cullum, J. Horizontal gene transfer and gene conversion drive evolution of modular polyketide synthases. *J. Ind. Microbiol. Biotechnol.* **39**, 1541–1547 (2012).
29. Medema, M. H., Cimermancic, P., Sali, A., Takano, E. & Fischbach, M. A. A systematic computational analysis of biosynthetic gene cluster

evolution: Lessons for engineering biosynthesis. *PLoS Comput. Biol.* **10**, e1004016 (2014).
30. Nivina, A., Paredes, S. H., Fraser, H. B. & Khosla, C. GRINS: genetic elements that recode assembly-line polyketide synthases and accelerate their diversification. *Proc. Natl. Acad. Sci. USA* **118**, e2100751118 (2021).
31. Zhang, B. et al. A type I/type III PKS hybrid generates cinnamomycin A-D. *Org. Lett.* **25**, 2560–2564 (2023).
32. Ser, H.-L. et al. Presence of antioxidative agent, Pyrrolo[1,2-a] pyrazine-1,4-dione, hexahydro- in newly isolated *Streptomyces mangrovisoli sp. nov*. *Front. Microbiol.* **6**, 854 (2015).
33. Latham, J. et al. Development of halogenase enzymes for use in synthesis. *Chem. Rev.* **118**, 232–269 (2018).
34. Yuzawa, S. et al. Comprehensive in vitro analysis of acyltransferase domain exchanges in modular polyketide synthases and its application for short-chain ketone production. *ACS Synth. Biol.* **6**, 139–147 (2017).
35. Wang, J. et al. Metabolic network model guided engineering ethylmalonyl-CoA pathway to improve ascomycin production in *Streptomyces hygroscopicus* var. *ascomyceticus*. *Microb. Cell. Fact.* **16**, 169 (2017). 31.
36. Myronovskyi, M. & Luzhetskyy, A. Native and engineered promoters in natural product discovery. *Nat. Prod. Rep.* **33**, 1006–1019 (2016).
37. Chen, A. Y. et al. Extender unit and acyl carrier protein specificity of ketosynthase domains of the 6-deoxyerythronolide B synthase. *J. Am. Chem. Soc.* **128**, 3067–3074 (2006).
38. Klaus, M., Buyachuihan, L. & Grininger, M. Ketosynthase domain constrains the design of polyketide synthases. *ACS Chem. Biol.* **15**, 2422–2432 (2020).
39. Yi, D. et al. Gatekeeping ketosynthases dictate initiation of assembly line biosynthesis of pyrrolic polyketides. *J. Am. Chem. Soc.* **143**, 7617–7622 (2021).
40. Hirsch, M., Fitzgerald, B. J. & Keatinge-Clay, A. T. How *cis*-acyltransferase assembly-line ketosynthases gatekeep for processed polyketide intermediates. *ACS Chem. Biol.* **16**, 2515–2526 (2021).
41. Wong, F. T. et al. Protein-protein recognition between acyltransferases and acyl carrier proteins in multimodular polyketide synthases. *Biochemistry* **49**, 95–102 (2010).
42. Lohman, J. R. et al. Structural and evolutionary relationships of "AT-less" type I polyketide synthase ketosynthases. *Proc. Natl. Acad. Sci. USA* **112**, 12693–12698 (2015).
43. Murphy, A. C. et al. Broadening substrate specificity of a chain-extending ketosynthase through a single active-site mutation. *Chem. Commun.* **52**, 8373–8376 (2016).
44. Butler, M. S., Robertson, A. A. & Cooper, M. A. Natural product and natural product derived drugs in clinical trials. *Nat. Prod. Rep.* **31**, 1612–1661 (2014).
45. McDaniel, R. et al. Multiple genetic modifications of the erythromycin polyketide synthase to produce a library of novel "unnatural" natural products. *Proc. Natl. Acad. Sci. USA* **96**, 1846–1851 (1999).
46. Smith, H. G., Beech, M. J., Lewandowski, J. R., Challis, G. L. & Jenner, M. Docking domain-mediated subunit interactions in natural product megasynth(et)ases. *J. Ind. Microbiol. Biotechnol.* **48**, kuab018 (2021).
47. Pourmasoumi, F. et al. Proof-reading thioesterase boosts activity of engineered nonribosomal peptide synthetase. *ACS Chem. Biol.* **17**, 2382–2388 (2022).
48. Peng, H. et al. Controlling substrate- and stereospecificity of condensation domains in nonribosomal peptide synthetases. *ACS Chem. Biol.* **19**, 599–606 (2024).
49. Scherlach, K. & Hertweck, C. Mining and unearthing hidden biosynthetic potential. *Nat. Commun.* **12**, 3864 (2021).
50. Wang, Z. et al. A naturally inspired antibiotic to target multidrug-resistant pathogens. *Nature* **601**, 606–611 (2022).

Acknowledgements

This work was supported by the grants of the Project Program of the State Key Laboratory of Natural Medicines, China Pharmaceutical University (SKLNMZZ2024JS06), National Key Research and Development Program of China (No.2018YFA0902000), Key Research and Development Project of Guangdong Province (2022B1111070004) and the "Double First-Class" University Project of China Pharmaceutical University (CPU2022QZ08).

Author contributions

W.J.: design, data curation, formal analysis, methodology and writing–original draft. J.T.: data curation, formal analysis. B.Z.: data curation, methodology. X.W.: resources, supervision. Y.C.: conceptualization, funding acquisition, supervision and writing–review and editing.

Competing interests

A Chinese patent application was filed with the number of 2024112777429. Y.C. and W.J. are the inventors of the patent, and China Pharmaceutical University owns the patent rights. All other authors declare no competing interests.

Additional information

Supplementary information The online version contains supplementary material available at https://doi.org/10.1038/s42004-025-01671-3.

Correspondence and requests for materials should be addressed to Yijun Chen.

Peer review information *Communications Chemistry* thanks Yuhui Sun and the other, anonymous, review for their contribution to the peer review of this work. Peer review reports are available.